Egyptian Journal of Pure and Applied Science

Use of Synthesized Aromatic Polyamide Reverse Osmosis Membranes Doped NanoTiO_2 in Water Desalination

Moustafa Mohamed Abo El-Fadl, Abdel-Hamid Mostafa El-Aassar*, Magdy Hosny El-Sayed, Mohamed Abdel Fatah El-Sheikh

Hydrogeochemistry Department, Desert Research Center, Cairo P.O.B. 11753 Egypt

A R T I C L E I N F O

Article history:
Received 12 July 2011
Accepted 25 September 2011

Keywords:
Aromatic polyamide;
Reverse Osmosis performance;
Desalination;
Transport mechanism.

A B S T R A C T

This paper reports an experimental study on reverse osmosis (RO) desalination of natural water samples using synthesized polyamide-grafted acrylic acid-titanium dioxide (PA-g-AAc-TiO_2) nanocomposite membrane. The phase inversion method with chemical initiation technique was used in the membrane synthesis. The behaviour of cations, anions and the hypothetical salts during the desalination process was studied. Also, the transport mechanisms of the different salts through the selected membrane were investigated. The obtained results showed that the electrical conductivity (EC) as well as the total dissolved solids (TDS) decrease as a function of operation time; the divalent cations and/or anions are more rejected than that of monovalent ions. Also, the hypothetical salts of brackish, saline groundwater and seawater samples are not changed after the desalination process. For brackish groundwater, the sequence of salts rejection related to initial concentration of each salt was arranged as: R_s $MgSO_4$, R_s $MgCl_2$ > R_s $CaSO_4$ > R_s Ca $(HCO_3)_2$ >R_s NaCl; while it was R_s $CaSO_4$ > R_s $MgCl_2$ > R_s $CaCl_2$, R_s $Ca(HCO_3)_2$ > R_s NaCl and R_s $MgCl_2$ > R_s $CaSO_4$, R_s $Ca(HCO_3)_2$ > R_s NaCl > R_s $MgSO_4$ for saline groundwater and seawater sample, respectively. The results obtained were in agreement with the coupled transport mechanism across the selected membranes.

Introduction

In Egypt, the desert region constitutes more than 96% of the total area of the country. The other 4% of the area include mainly the cultivated lands in the Nile valley and Delta where the majority of Egyptian population is concentrated and less than 5% of the population are scattered in all desert areas. It is well known that the water resources in Egypt are limited. Meanwhile, water demand is continually increasing due to population growth, industrial development and the increase of living standards. Because of population growth, the per capita share of water has dropped dramatically to less than 1000 m^3/capita, which, by international standards, is considered the "Water Poverty Limit". The value may even decrease to 500 m^3/capita in the year 2025. This urged the successive governments to draw various programs for land reclamation in desert areas. Such programs, mostly, depend totally or partially on local groundwater resources in desert areas and the development of non-conventional water resources such as reuse of water and desalination of saline water. Sinai represents 6 % of the total area of Egypt. Overall integrated development of Sinai necessitates linking the east side of the Suez Canal with the western side and providing it with water source; so water desalination became the main water source in this important area[1]. El-Maghara area, middle Sinai-Egypt, is considered as an example of arid zone which suffer from high salinity groundwater and shortage of water resources. The study area lies between longitudes 33^o 10' - 33^o 40' E and latitudes 30^o 35' - 30^o 50' N and covers about 1500 Km^2. It lies about 182 km to the northeast of El-Ismailia city and 120 km to the southwest of El-Arish city, Fig. (1).

The applicability of membrane separations for water treatment is well known. Membrane separation technology has been widely used for desalination of sea and brackish waters[2-4]. The reverse osmosis (RO) process which uses polymeric membranes to achieve molecular separation excels all other methods of desalination and is considered as the simplest and most efficient technique to desalt saline/seawater[5]. For development of these polymeric RO membranes, two

* Corresponding author.
E-mail address: hameed_m50@yahoo.com
Tel. fax: (202)26389069

different techniques have been used: the phase inversion method for asymmetric membranes, and the interfacial polymerization for thin film composite (TFC) membranes[6-8]. In recent years, titanium dioxide (TiO_2) nano-particles have received much attention because of its important role in various applications[9,10]; it has been applied to a variety of problems of environmental interest in addition to water and air purification[11,12].

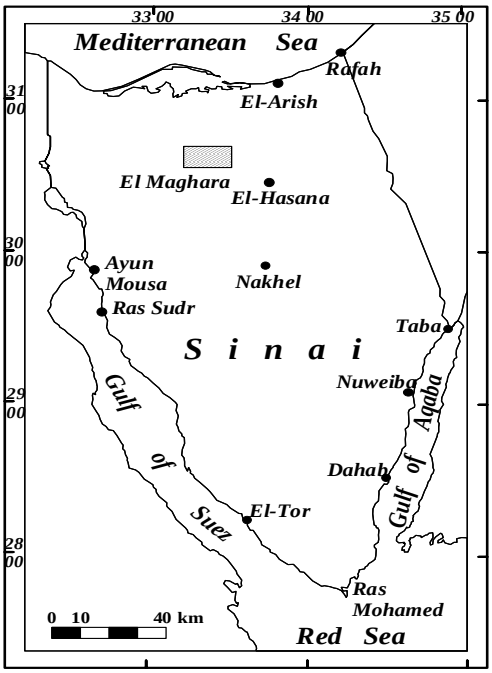

Fig. 1: Location map of the study area.

Reverse osmosis performance parameters, salt rejection and permeate flux, are known to be influenced by membrane characteristics, by physicochemical properties of the system, and by operating variables such as solute concentration and operating pressure[4]. In order to maximize the solute separation ability and efficiency, one has to develop membranes from available polymers having suitable pore size combined with an appropriate chemical nature of the polymer[5]. In RO processes, preferential sorption at membrane-solution interface is one of the factors governing solute separation. It is a function of the membrane material, solute and solvent interactions together with the experimental conditions. These interactions arise in general from the ionic, steric, polar and/or non-polar character of each one of the above three components of the system involved. Two essential membrane parameters in the RO process are solubility and diffusivity of solutes and solvents to the active-layer polymers[13,14], which determine the membrane rejection and the flux. The inter-relationships between the RO membrane rejection and the polymer–solute/–solvent interactions, in conjunction with the chemical structure of the active-layer polymers, have been considerably studied[11,15].

The aim of this work is to apply the best of some synthesized RO aromatic polyamide membranes in desalination of Red sea and two groundwater samples collected from El-Maghara area, middle Sinai, Egypt.

Experimental procedures

1. Materials:

Poly [(m-phenylene isophthalamide)] [PMPIPA] and N, N-Dimethyl acetamide (DMAc) were supplied by Aldrich. Acrylic acid (AAc), purity 99.9% was used as received and purchased from Merck, Germany. Titanium dioxide nano-particles (TiO_2) in its commercial form (P25, 80% anatase, 20% rutile, BET area 50m^2/gm, 30) was obtained from Deggusa. Sodium dodecyl sulfate (SDS) was used as surfactant; the other chemicals such as solvents and inorganic salts were reagent grade and used without any further purification.

2. Membrane preparation:

Different membranes of polyamide un-grafted, AAc grafted and/or modified with TiO_2 nanoparticles were prepared. The polymer with 7wt.% concentration was dissolved using DMAc as a solvent and LiCl as inorganic additives until complete dissolving of polymer and forming the casting solution. For (PA-g-AAc) membrane, the chemical initiation process was used with benzoyl peroxide (BPO) as a chemical initiator. The monomer concentration represents 20 wt. % of polymer, BPO concentration was 5 wt. % of monomer, the desired temperature and time which required for complete the reaction was 85°C for 120 min, respectively. For (PA-g-AAc/TiO_2), TiO_2 nano-particles are firstly modified with sodium dodecyl sulfate (SDS) as a surfactant to prevent any aggregation of nano-particles in the membrane matrix. Where, 1g of TiO_2 nano-particles was added to 0.7 % SDS at adjusted pH 4 with nitric acid, then stirred for 6h and the modified TiO_2 was obtained by centrifuge, then dried at 60°C for 24 h; TiO_2 with 3wt. % was added to the casting solution before the chemical initiation process. The solutions were casted on a glass plates, then allowed to dry to obtain the membranes. After this process the membranes were immersed in a coagulation bath of distilled water for about 12h at 25°C (complete exchange of solvent). After precipitation, the membranes were washed in distilled water and dried completely in a vacuum system or kept in distilled water until its application in water desalination process.

3. Water Analyses

Water analyses include the determination of EC, total dissolved solids (TDS), pH, concentration of major ions Ca^{2+}, Mg^{2+}, Na^{+}, K^{+}, CO_3^{2-}, HCO_3^{-}, SO_4^{2-} and Cl^{-}. All the analyses were done according to Rainwater and Thatcher, 1960[16], Fishman and Friedman, 1985[17], and ASTM, 2002[18]. Measurements were carried out by EC meter model Orion (150 A^{+}), pH meter (Jenway 3510), Flame photometer (Jenway PFP 7), and UV/Visible spectrophotometer. The obtained chemical data are expressed in milligram per liter (mg/l), part per million (ppm) and equivalent part per million (epm).

4. RO Performance:

Reverse osmosis properties (salt rejection and permeate flux) of the synthesized membranes were measured by

laboratory DDS reverse osmosis system, model LAB-M20, manufactured by Alfa Laval Comp., Denmark. It consists of stainless steel cylindrical vessel, 20cm in diameter and 70cm height, with control panel. The effective membrane areas range from 0.036 to 0.72 m^2 (0.018m^2 per membrane). The salt rejection percent (R_s %) was calculated as: R_s (%) = (C_f - C_p/C_f) x 100, where C_f and C_p are the concentrations of feed and permeate water (product), respectively.

The water flux through a semi-permeable membrane is expressed in weight of the product (grams) per unit membrane area (cm^2) during operation time in sec.

Results and Discussion

By studying RO performance of different synthesized PA, PA-g-AAc and PA-g-AAc/TiO_2 membranes and comparison their salt rejection (%) and permeate flux, at the same operation conditions which include NaCl as feed solution with EC 20000 µmhos, applied pressure 30 bar, 5L/min flow rate for 8h operation time at room temperature, the result investigated indicate that the synthesized PA-g-AAc/TiO_2 nanocomposite membrane possess the highest water flux (J_w= 34 g/cm^2.sec×10^{-5}) with acceptable salt rejection (R_s= 42 %), Fig. (2). Therefore, this membrane was selected for water desalination process.

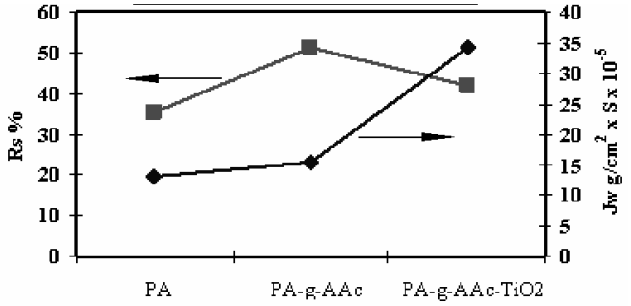

Fig. 2: RO performance for different synthesized membranes.

Brackish groundwater (TDS: 3333 ppm), saline groundwater (TDS: 13986 ppm) and the Red sea (TDS: 42847 ppm) water samples were pumped into the RO unit as feed solutions using 30, 40 and 50 bar applied pressures, respectively, against the selected membrane. Feed and permeate salinity of each sample were determined up to 24 hours. The obtained results show that EC and TDS decrease as a function of operation time, Fig. (3).

Also, the concentration of major constituents was measured to study the behaviour of cations, anions and the hypothetical salts.

1. Behaviour of cations, anions and the hypothetical salts during the desalination process:

The behaviour of cations and anions during the desalination process can be written according to the sequence of rejection percentage of cations as: R_s Mg^{2+} > R_s Ca^{2+} > R_s Na^+ for all water samples. While the anions sequence was: R_s SO_4^{2-}>R_s HCO_3^- > R_s Cl^- for both brackish and saline groundwater samples and: R_s Cl^- > R_s SO_4^{2-}>R_s HCO_3^- for sea water, Figs. (4-6).

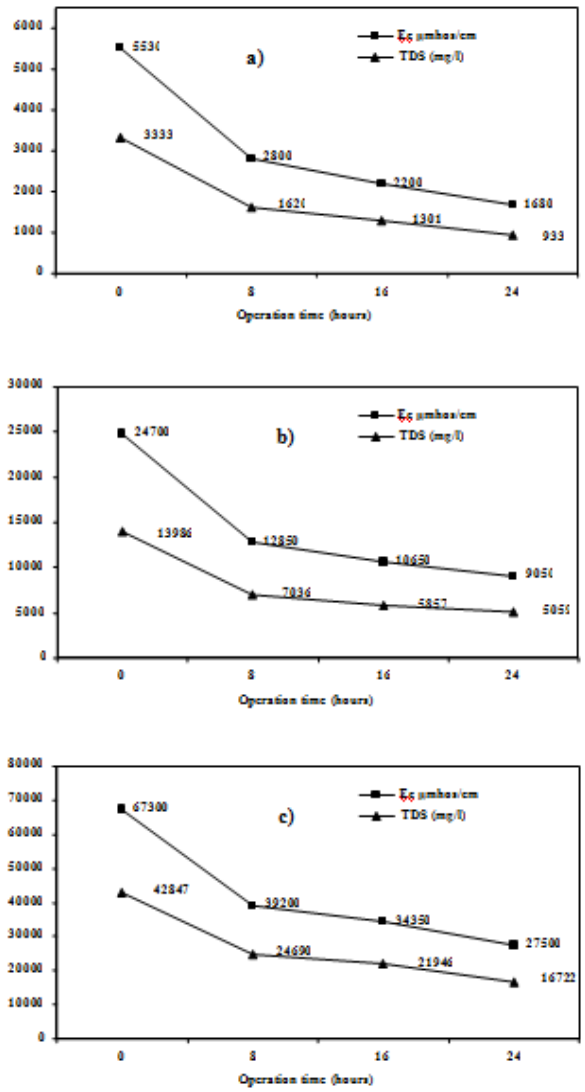

Fig. 3: EC and TDS as a function of operation time during desalination process of (a) brackish, (b) saline groundwater and (c) seawater samples.

Generally, it was noted that, the divalent cations and/or anions are more rejected than that monovalent. The only difference between sea water and the other water samples was the order of the anions rejection sequence. Also, the hypothetical salts of the different water samples are not changed during and after the desalination process i.e., the pre- and post treated water have the same hypothetical salt types. The changes are related to its percentage (%) regarding to TDS.

For brackish groundwater sample, the hypothetical salts were NaCl, $MgCl_2$, $MgSO_4$, $CaSO_4$ and Ca $(HCO_3)_2$. The sequence of salts rejection related to the initial concentration of each salt can be arranged as: R_s $MgSO_4$, R_s $MgCl_2$ > R_s $CaSO_4$ > R_s Ca $(HCO_3)_2$ >R_s NaCl, Fig. (7).

The membrane showed high rejection for magnesium salts ($MgSO_4$, $MgCl_2$), moderate rejection for calcium salts [$CaSO_4$, Ca $(HCO_3)_2$] and low rejection for NaCl salt. Table (1) shows the water flux and salt rejection (%) of the hypothetical salts as a function of the operation time.

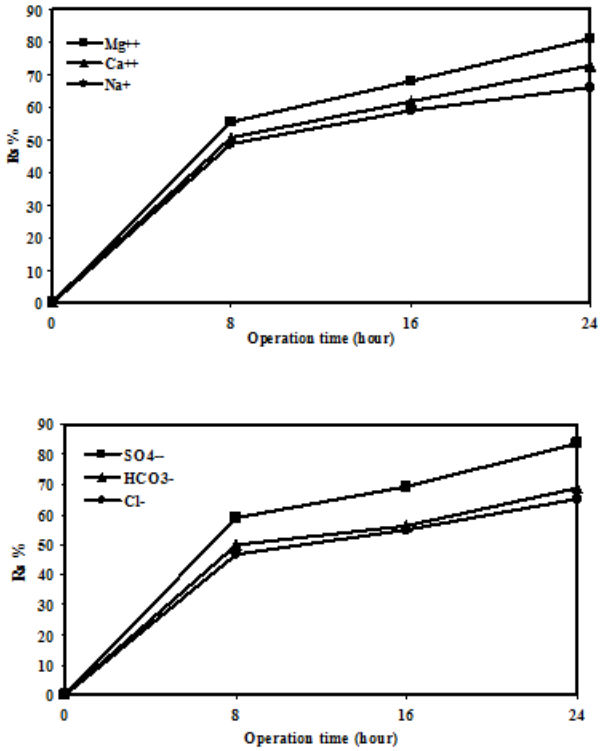

Fig. 4: Behaviour of major ions during desalination of brackish groundwater sample.

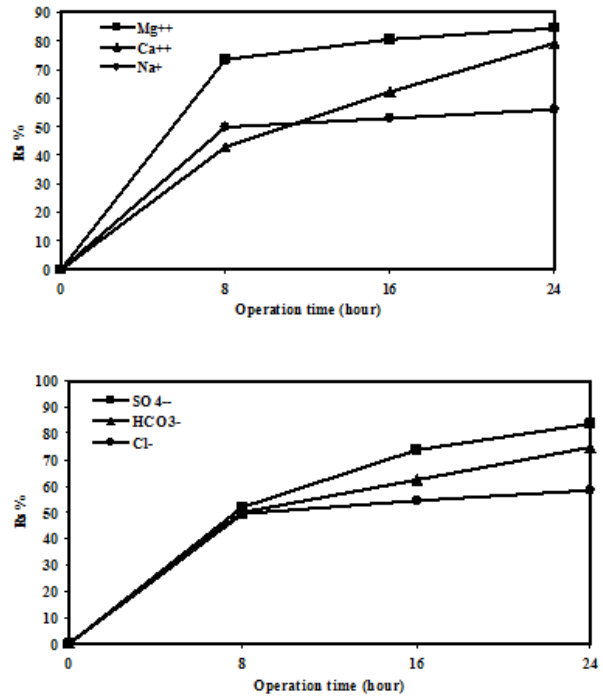

Fig. 5: Behaviour of major ions during desalination of saline groundwater sample.

While for saline groundwater; the hypothetical salts were NaCl, $MgCl_2$, $CaCl_2$, $CaSO_4$ and $Ca(HCO_3)_2$. The sequence of salt rejection related to initial concentration of each salt can be arranged as: R_s $CaSO_4$ > R_s $MgCl_2$ > R_s $CaCl_2$, R_s $Ca(HCO_3)_2$ > R_s NaCl, Fig. (8) and Table 2

The membrane has shown high rejection for Ca and Mg salts [$CaSO_4$, $MgCl_2$, $CaCl_2$, Ca $(HCO_3)_2$] and moderate rejection for NaCl salt.

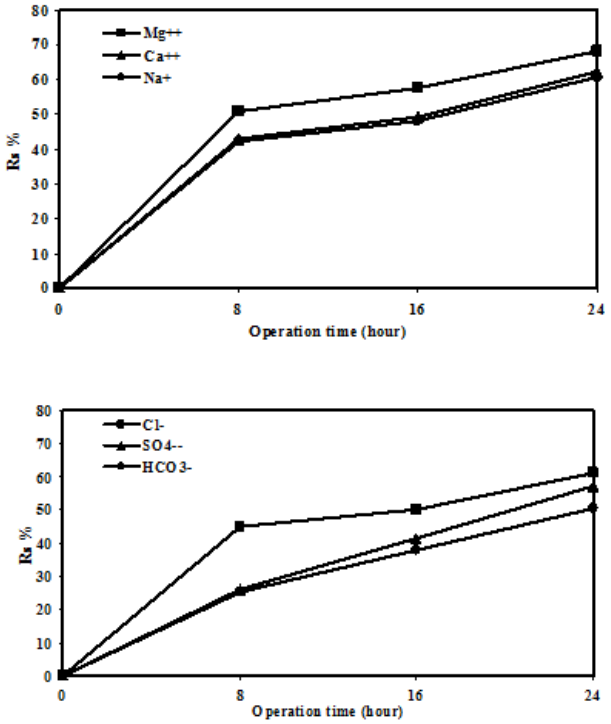

Fig. 6: Behaviour of major ions during desalination of seawater sample.

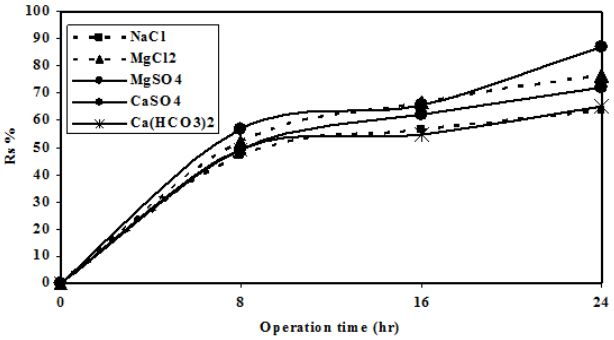

Fig. 7: Behaviour of the hypothetical salts during desalination of brackish groundwater sample.

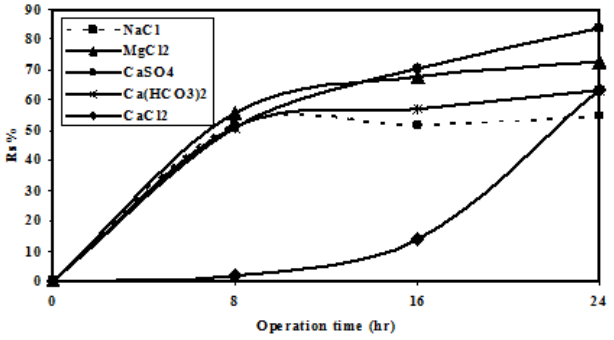

Fig. 8: Behaviour of the hypothetical salts during desalination of saline groundwater sample.

Table (1): Reverse osmosis parameters for the selected membrane in desalination of brackish water sample

Time (hr.)	Feed conc. (ppm)	Post treatment water (ppm)	$J_w x10^{-5}$ (gm/cm^2.s)	R_S (%)	Salt rejection (%)				
					NaCl	$MgCl_2$	$MgSO_4$	CaSO4	$Ca(HCO_3)_2$
8	3333	1619.9	15.43	51	22.67	9.74	4.08	11.31	3.60
16		1301.4	14.20	61	26.47	12.14	4.66	13.80	3.88
24		933	10.28	72	30.60	14.08	6.16	16.40	4.76

Table (2): Reverse osmosis parameters for the selected membranes in desalination of saline groundwater sample

Time (hr.)	Feed conc. (ppm)	Post treatment water (ppm)	$J_w x10^{-5}$ (gm/cm^2.s)	R_S (%)	Salt rejection (%)				
					NaCl	$MgCl_2$	$CaCl_2$	$CaSO_4$	$Ca(HCO_3)_2$
8	13986	7036	13.88	48.00	29.11	10.22	-0.02	7.70	0.99
16		5856	10.80	57.00	31.05	13.00	0.49	11.30	1.16
24		5059	9.26	63.00	32.17	14.17	1.91	13.47	1.28

Table (3): Reverse osmosis parameters for the selected membranes in desalination of seawater sample

Time (hr.)	Feed conc. (ppm)	Post treatment water (ppm)	$J_w x10^{-5}$ gm/cm^2.s)	R_S (%)	Salt rejection (%)				
					NaCl	$MgCl_2$	$MgSO_4$	$CaSO_4$	$Ca(HCO_3)_2$
8	42847	24689	12.85	42.00	30.52	8.12	1.66	1.27	0.42
16		21946	11.82	49.00	36.24	8.44	2.37	1.46	0.49
24		16721	8.18	59.00	44.33	8.13	4.10	1.83	0.61

Table (4): Diffusivities, stokes radii and hydration energy of the major ions.

Ion	D_s ($10^{-9}m^2.sec^{-1}$)	r_s (nm)	Hydration energy ($kJ.mol^{-1}$) a
Na^+	1.333	0.183	407
Mg^{2+}	0.706	0.345	1921
Ca^{2+}	0.92	0.307	1584
Cl^-	2.032	0.12	376
HCO_3^-	1.85	0.167	--
SO_4^{2-}	1.065	0.229	1138

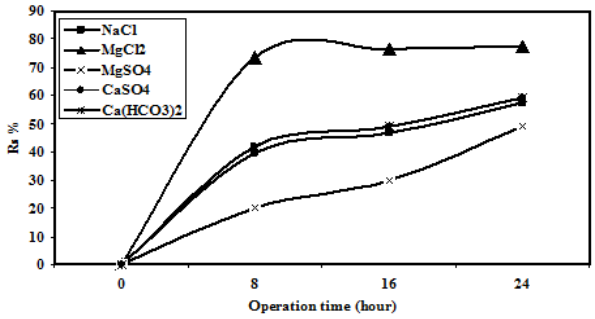

Fig. 9: Behaviour of the hypothetical salts during desalination of seawater sample.

Also, the desalination process does not change the hypothetical salts in both pre- and post-treated waters for sea water sample which have the same types of salts: NaCl, $MgCl_2$, $MgSO_4$, $CaSO_4$ and $Ca(HCO_3)_2$. The sequence of salts rejection related to the initial concentration of each salt can be arranged as: R_s $MgCl_2$ > R_s $CaSO_4$, R_s Ca $(HCO_3)_2$ > R_s NaCl > R_s $MgSO_4$, Fig. (9) and Table (3). The membrane displayed high rejections for chloride, sulfate and bicarbonate salts of divalent cations [Mg Cl_2, $CaSO_4$ and Ca $(HCO_3)_2$] and moderate rejections for NaCl and $MgSO_4$.

From the obtained data, the salt rejection (%) increases with increasing operation time, while the water flux decreases. This is due to the fact that as the operation time increases the accumulation of salts in the pores of membrane is produced; this resulted in reducing the water flux and increasing the salt rejection. Also, the selected nano-composite membrane (PA-g-AAc/TiO_2) could be acceptable for practical uses in RO desalination of brackish, saline and sea water samples. This is due to high water flux and salt rejection. The salt rejection (%) was 70, 63 and 59 %, after 24h. operation time, for brackish, saline and seawater samples, respectively, with acceptable water flux.

However, to understand the behaviour of cations, anions and the hypothetical salts during the water desalination process, the possible mechanisms for the separation of multi-component electrolytes using a membrane and the

interactions between membrane material, solute and solvent are discussed[19]; these are:

1. Sieving (depending on ionic radii).
2. Electrostatic interactions between the membrane and ions or between ions mutually.
3. Differences in diffusivity and hydration energy of ions.

According to the sieving mechanism and the values of ionic radii for both cations and anions, Table 4, the cationic radii are decreased in the order $r_s\ Mg^{2+} > r_s Ca^{2+} > r_s\ Na^+$; this reflects the rejection of cations is in the order $R_s\ Mg^{2+} > R_s\ Ca^{2+} > R_s\ Na^+$. Also the anionic radii are decreased in the order $r_s\ SO_4^{2-} > r_s\ HCO_3^- > r_s\ Cl^-$, reflecting the rejection in the order $R_s\ SO_4^{2-} > R_s\ HCO_3^- > R_s\ Cl^-$.

According the electrostatic interaction mechanism which deals with the interaction between the membrane surface and the ions in solution, it is expected that the electrostatic repulsion will help make in repelling of different species of anions by the charged membranes. It is important to mention that TiO_2 is an amphoteric oxide with an iso-electric point (IEP) of 6. Therefore, when the solution pH is higher than the IEP of TiO_2, the TiO_2 surface is negatively charged[20]. In other words, the presence of COO^- and TiO_2 on the membrane surface makes the surface negatively charged. These negative charges undergo repulsion with the anion species in the electrolyte solution according to the Donnan exclusion mechanism[21]. In this mechanism, the co-ions (which have the same charge of the membrane) are repulsed by the membrane surface charge and to satisfy the electro-neutrality condition, an equivalent number of counter-ions (which have the opposite charge of the membrane) is retained which resulted in salt rejection. On the basis of Donnan exclusion theory, a high co-ion valency causes a higher salt rejection. So, beside the effect of ionic radii, the rejection can be written in the order: $R_s\ SO_4^{2-} > R_s\ HCO_3^- > R_s\ Cl^-$ and $R_s\ Mg^{2+} > R_s\ Ca^{2+} > R_s\ Na^+$ based on repulsion and attraction forces, respectively. Usually, large size solutes (salts of Ca^{2+} and Mg^{2+} ions) with higher charges show a high rejection[22]. In case of $MgSO_4$, $MgCl_2$, $CaSO_4$ and $Ca(HCO_3)_2$ salts; there is strong adsorption of Mg^{2+} and Ca^{2+} ions. This could explain the fact that these salts are better rejected than NaCl.

Based on the difference in diffusivity of different ions in the solution, for ions of the same valence (cations or anions), the rejection sequence could be affected according to the difference in ion diffusivities. Indeed, as shown in table (4), the sequence of ion diffusivities is $D_s\ (Na^+) > D_s\ (Mg^{2+}) > D_s\ (Ca^{2+})$, is inversely reflected in the rejection sequence[23]. Also, for anions the sequence of ion diffusivities is $D_s\ Cl^- > D_s\ HCO_3^- > D_s\ SO_4^{2-}$, while the rejection sequence is $R_s\ Cl^- > R_s\ HCO_3^- > R_s\ SO_4^{2-}$.

On the other hand, the hydration energy plays an importance role in rejection process of ions, i.e. the ion with strong hydration energy is reduced in the permeability through the membrane as compared to that with low hydration energy[24].

The hydration energy of the cations is decrease in the order $E_h\ Mg^{2+} > E_h\ Ca^{2+} > E_h\ Na^+$. As a result, the rejection is in the order $R_s\ Mg^{2+} > R_s\ Ca^{2+} > R_s\ Na^+$. For anions the hydration energy is decreased in the order $E_h\ SO_4^{2-} > E_h\ HCO_3^- > E_h\ Cl^-$; as a result, the rejection is in the order $R_s\ SO_4^{2-} > R_s\ HCO_3^- > R_s\ Cl^-$. The cationic rejection sequence can be explained on basis of difference in stock radii, ion diffusivity and hydration energy of different cations as motioned before. Nevertheless, the anionic rejection sequence at the high concentration of feed solution cannot be explained according to the same hypothesis. Wang et al.[25] suggested that the steric hindrance effect is the major factor of the salt rejection. According to the electrostatic and steric hindrance (ES) model, the steric hindrance effect increases with increasing the ratio of solute Stocks radius to pore radius. The sequence of Stocks radii for cations is: $r_s\ (Mg^{2+}) > r_s\ (Ca^{2+}) > r_s\ Na^+$. So, the rejection sequence of cations is $R_s\ (Mg^{2+}) > R_s\ (Ca^{2+}) > R_s\ Na^+$. But in case of anions, the sequence of rejection cannot be explained by ES model because r_s of Cl^- is smaller than those of sulfate and bicarbonate. This behavior may be explained on the basis of high concentration of Cl^- ions in seawater relative to other ions.

According to the difference in diffusivity coefficient between the different salts, the salt with the lowest diffusion coefficient shows the highest rejection, whereas that with the highest diffusion coefficient shows the lowest rejection[24]. Although the mentioned three mechanisms discussed the behaviour of cations, anions and the hypothetical salts during the desalination process, it did not identify the rejection taking place by ions or salts. Therefore, the following solution-diffusion model was discussed.

2. Transport mechanism through the selected membrane:

For RO membranes, the solution-diffusion mechanism has been widely used to characterize the transport of solvent and permeating solutes through the active asymmetric membrane[26].

Electrolyte transport through RO membrane may occur through two distinctly different pathways: (i) ion pair mechanism and (ii) coupled transport of ions. For the ion pair mechanism, cations and anions associate to form electrically neutral ion pairs at high electrolyte concentration near the membrane-water interface due to the concentration polarization effect. Subsequently, ion pairs get partitioned into relatively non-polar asymmetric layers of membrane and permeate to the low pressure side. By varying feed concentration (C_f) and trans-membrane pressure for a single electrolyte, the salt concentration permeate (C_p) varies according to the ion pair mechanism: $C_p = \text{constant } (C_f)^2$ ------- (1)

For the coupled transport mechanism, the membrane phase can be considered to be adequately solvated due to the trans-membrane transport of polar water molecu-

les. Thus, individual ions (not ion pairs) get partitioned into the solvent permeated membrane and migrate to the permeate side in a manner that the negative charge of an ion is balanced by the equivalent positive charge of an accompanying cation. The inter-diffusion coefficient of the electrolyte governs the permeation rate according to the coupled transport mechanism:

C_p= constant (C_f) ------ (2)

On a logarithm-logarithm scale, the plots of equations (1) and (2) for the two proposed mechanisms take the following forms:

For ion- pair mechanism:

Log C_p= constant + 2 log (C_f)------(3)

For coupled ions mechanism:

Log C_p= constant + log (C_f)--------(4)

The distinction between equations (3) and (4) can be readily noted. The salt concentration in permeate is linearly dependent on the feed concentration according to the coupled transport mechanism while permeate salt concentration varies with the square of the feed concentration according to ion-pair mechanism. Thus, C_p versus C_f plot on a log-log scale will yield a slope of 2 and 1 according to ion-pair mechanism and coupled ion transport mechanism, respectively.

The mechanism of electrolyte transport through the selected membranes should be dependent of the valence of constituent cations and anions which represent the major components of the three water samples having different concentrations. That is why experimental data were collected to groundwater and seawater samples, which include four salts of different valences e.g. NaCl (1:1), $MgCl_2$ (2:1), $MgSO_4$ (2:2), $CaSO_4$ (2:2) and $Ca(HCO_3)_2$ (2:1).

Figure (10) shows log C_p versus log C_f plots from a series of runs carried out using the selected membrane in desalination of different feed concentrations (C_f: 3333, 13986 and 42847 mg/l) of water samples; water flux and operation times were kept nearly constant by altering feed pressures. The different salts permeate sequence can be arranged in the order; NaCl > $CaSO_4$ ≈ $MgCl_2$> Ca $(HCO_3)_2$.

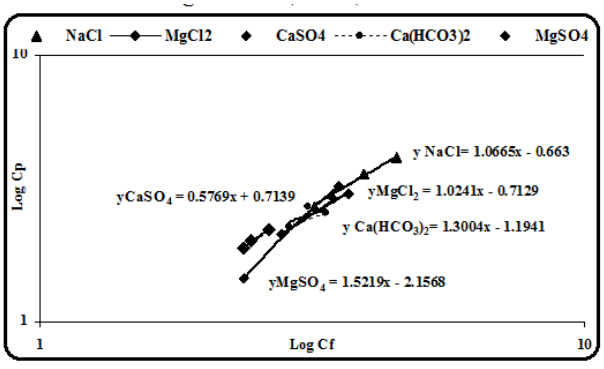

Fig. 10: Plots of log C_p Vs. log C_f of different salts for RO runs using the three different water samples.

Permeates of sulfate, chloride and bicarbonate salts for divalent cations are lower than that of NaCl permeate under identical conditions. With an increase in feed concentration (C_f) at nearly constant water flux (J_w), salt concentrations in the permeate increase. This agrees well with the already mentioned results obtained from the desalination of the three water samples. However, the slopes of log C_p versus log C_f plots for the different salts present such as NaCl (1:1), $MgCl_2$ (2:1), $MgSO_4$ (2:2), $CaSO_4$ (2:2) and Ca $(HCO_3)_2$ (2:1) were close to unity. This is in agreement with the prediction of coupled transport mechanism across PA-g-AAc/TiO_2 RO membranes.

Conclusions

A series of some RO aromatic polyamide membranes were prepared using phase inversion method with the chemical initiation technique. By studying the RO performance of the different synthesized PA, PA-g-AAc and PA-g-AAc/TiO_2 membranes and comparison according to the values of their salt rejection (%) and flux using NaCl as feed solution, PA-g-AAc/TiO_2 nano-composite membrane was selected for desalination of brackish and saline waters.

Red sea and two groundwater samples were collected from El-Maghara area, middle Sinai, Egypt. The behaviour and the transport mechanism of the different salt types involving mono and divalent cations and anions were studied. The obtained results lead to the following general conclusion:

(1) The EC as well as TDS decrease gradually as a function of operation time.

(2) The divalent cations and/or anions are more rejected than that of monovalent ions. Also, the hypothetical salts of the tested samples do not change after the desalination process.

(3) For brackish groundwater, the sequence of salts rejection related to is initial concentration of each salt is arranged as: R_s $MgSO_4$, R_s $MgCl_2$ > R_s $CaSO_4$ > R_s $Ca(HCO_3)_2$ >R_s NaCl; while it was R_s $CaSO_4$ > R_s $MgCl_2$ > R_s $CaCl_2$; R_s $Ca(HCO_3)_2$ > R_s NaCl and R_s $MgCl_2$ > R_s $CaSO_4$, R_s $Ca(HCO_3)_2$ > R_s NaCl > R_s $MgSO_4$ for saline groundwater and sea water sample, respectively.

(4) The slopes of log C_p versus log C_f plots for the different salts present such as NaCl (1:1), Mg Cl_2 (2:1), Mg SO_4 (2:2), $CaSO_4$ (2:2) and Ca $(HCO_3)_2$ (2:1) were close to unity. This is in agreement with the prediction of coupled transport mechanism across PA-g-AAc/TiO2 RO membrane.

References

1) A. Hafez, "Investigation of Al-Salam canal project in northern Sinai, Egypt, Phase-I: Environmental baseline, soil and water quality studies", Ninth International Water Technology Conference, IWTC9 2005, Sharm El-Sheikh, Egypt.

2) G. Belfort, "Synthetic Membrane Processes, Fundamentals and Water Applications", Academic Press, Orlando, FL, 1984.

3) S. Sourirajan, T. Matsuura, "Reverse Osmosis/Ultra filtration Process Principles", National Research Council Canada, Ottawa, 1985, pp. 848–884.

4) K. Košuti´c, L. Kaštelan-Kunst, B. Kunst, "Porosity of some commercial reverse osmosis and nanofiltration polyamide thin-film composite membranes", j. of Membrane Science 168 (2000) 101.

5) A. P. Rao, N.V. Desai, R. Rangarajan, "Interfacially synthesized thin film composite RO membranes for seawater desalination", j. of Membrane Science 124 (1997) 263-272.

6) R.J. Petersen, "Composite reverse osmosis and nanofiltration membranes", J. Membrane Sci., 83 (1993) 81.

7) T. Matsuura, "Progress in membrane science and technology for seawater desalination-a review", Desalination, 134 (2001) 47.

8) B. J. Abu Tarbousha, D. Ranaa, T. Matsuura, H.A. Arafat, R.M. Narbaitzc, "Preparation of thin-film-composite polyamide membranes for desalination using novel hydrophilic surface modifying macromolecules", J. of Membrane Science, 325 (2008) 166–175.

9) N. Wu, M. S. Lee, "Enhanced TiO_2 photo-catalysis by Cu in hydrogen production from aqueous methanol solution", Internal. J. Hyd. Energy, 29 (2004)1601.

10) M. Keshmiri, M. Mohseni, T. Troezynski, "Development of novel TiO_2 sol-gel derived composite and its photo catalytic activities for trichloroethylene oxidation", Appl. Cat. B: Env., 53 (2004) 209.

11) H.G. Spencer, J.L. Gaddis. "Hyperfiltration of nonelectrolytes: dependence of rejection on solubility parameters", Desalination 1979; 28:117.

12) A. B. Yanan Yang, W. Peng "Preparation and characterizations of a new PS/TiO_2 hybrid membranes by sol–gel process", Polymer, 47 (2006), 2683.

13) T. Matsuura, "Synthetic Membranes and Membrane Separation Processes", CRC Press, Boca Raton, 1994.

14) S. Kwak, "Relationship of relaxation property to reverse osmosis permeability in aromatic polyamide thin-film-composite membranes", Polymer 40 (1999) 6361–6368.

15) P.Lipp, R.Gimbel, F.H. Frimmel, "Parameters influencing the rejection properties of FT30 membranes", J. Membrane Sci 1994; 95:185.

16) F. H. Rainwater, L. L. Thatcher, "Methods for collection and analysis of water samples" U.S. Geol. Survey. Water Supply, Paper No.1454, (1960), U.S.A. 301p.

17) M. J. Fishman, L. C. Friedman, "Methods for determination of inorganic substances in water and fluvial sediments "U.S. Geol. Surv. Book 5, Chapter A1. Open File Report, (1985), pp.85-495, Denver, Colorado, U.S.A.

18) Annual book of ASTM standards, U.S.A. Sec. 11, Vol.11.01, and 11.02, West Conshohocken.

19) J. M. Peeters J.P. Boom, M. H. Mulder, H. Strathmann, "Retention measurements of nano-filtration membranes with electrolyte solutions" J. Membrane Sci. 145, (1998), p 199.

20) F. Guifen, S. Patricia, C. Lin, "Anatase TiO_2 Nano-composites for Antimicrobial Coatings" J. Phys. Chem. B. Vol. 109 (2005), p 8889.

21) M. R. Teixeira, M. J. Rosa, M. Nystrom, ''The role of membrane charge on nano-filtration performance" J. Membrane. Sci. 265(2005), p 160.

22) J. Mo, S. Son, J. Jegal, J. Kim and Y. H. Lee, "Preparation and Characterization of Polyamide Nano-filtration Composite Membranes with TiO_2 Layers Chemically Connected to the Membrane Surface" J. Appl. Poly. Sci. l 105(2006), p 1267.

23) J. Schaep, C. Vandecasteele, A. W. Mohammad, W. R. Bowen, "Modeling the retention of ionic components for different nanofiltration membranes" Sep. and Purif. Tech. Vol. 22-23, (2001) 169-179.

24) H. M. Krieg, S. J. Modise, H. W. Keizer, J. P. Neomagus, "Salt: rejection in nanofiltration for single and binary salt mixtures in view of sulfate removal", Desalination, Vol. 171, (2004) pp 205-215.

25) X. L. Wang, T. Tsuru, M. Togoh, "Evaluation of pore structure and electrical properties of nanofiltration membranes " J. Chem. Eng. Vol 28, (1995) pp 186-192.

26) P. Mukherjee, A. K. SenGupta, "Some observation about electrolyte permeation mechanism through reverse osmosis and nanofiltration membranes", J. of membrane Sci. vol. 278, (2005), 301-307.